Proceedings of the 2005 IEEE/ASME
International Conference on Advanced Intelligent Mechatronics
Monterey, California, USA, 24-28 July, 2005

An Analytical Method for Design of Compliant Grippers with Macro/Micro Manipulation and Assembly Applications

Chao-Chieh Lan and Kok-Meng Lee

Abstract: **A compliant gripper gains its dextral manipulation by the flexural motion of its fingers. It is a preferable device to grippers with actuations because of reduced fabrication complexity and increased structural reliability. The prediction of contact forces and deflected shape are essential to the design of a compliant gripper. We present here a formulation based on Nonlinear Constrained Optimization (NCO) techniques to analyze contact problems of compliant grippers. For a planar compliant gripper this formulation essentially reduces the domain of discretization by one dimension. Hence it requires simpler formulation and is computationally more efficient than other methods such as finite element analysis. As this method is rather generic, its use will facilitate design analysis and optimization of compliant devices. We illustrate these attractive features with two types of compliant grippers; macro-handling and micro-assembly applications.**

Keywords –Flexible Manipulators; Micro Manipulation

1 Introduction

Mechanical grippers have many applications in high-speed production automation. A typical robotic gripper with two or more rigid fingers is often actuated by an electrical or a pneumatic motor. Unlike grippers with rigid fingers, a compliant gripper is capable of large flexural deflection and is manipulated by means of its contact with the object being handled rather than by an external actuator. The concept of compliant gripping has been widely used for snap-fit assembly. Bonenberger [1] has a comprehensive description on design of snap-fit assembly. Lee *et al* [2] designed the complaint rubber grippers for singulating broiders for poultry meat production, and later [3] exploited their application as graspers to automate transferring of live birds. As a compliant gripper requires no external actuators and sensors for feedback to accommodate a limited range of shapes/sizes of the live objects, it has been more attractive than traditional grippers for high-speed automation. In addition, compliant grippers are easy to fabricate, assemble, and maintain.

Advance in MEMS has realized the need for mass production of micro components. Various micromachining methods have been developed, such as IC-based silicon processing, LIGA, surface machining, and micro electro discharge machining (EDM). However, these techniques are only capable of two-dimensional (2D) fabrication. In order to create broader applications based on MEMS devices, it is required to develop microgrippers for manipulating and assembling micro components for 3D applications. The interest to reduce the complexity of 3D assembly has motivated the development of passive microgrippers. As compared to active microgrippers which may be driven by means of electro-thermal [4], electrostatic [5], electromagnetic [6] or piezoelectric [7] actuators, passive micro-grippers requiring no external actuators rely on contact between compliant fingers and the micro component to generate motion required for assembly; for examples, a micro-machined end-effector for MEMS assembly [8], and a compliant microgripper for micro snap-fit connector [9]. Since uncertain actuator displacement does not exist in passive microgrippers, they have significant potential for very high precision applications. However, design of a compliant gripper is more challenging due to the difficulty in predicting the contact-induced deflection of its fingers.

Compliant fingers undergo large deflection when they contact the object. The essence of the analysis is to determine the normal and tangential contact forces that must satisfy the boundary conditions at the interface. Since most contact problems involving large deformation do not permit analytical solutions, designers have resorted to numerical methods for approximation solutions. Among them, the *matrix inversion method* satisfies boundary conditions at specified matching points. It has been used by Paul & Hashemi [10] to calculate normal contact forces. Another method, the *variational inequality method,* determines the shape and size at contact by using well-developed optimization techniques. Fichera [11] and Duvant & Lions [12] have investigated on the existence and uniqueness of solution to contact problems. They show that the true contact area and surface displacement are those that minimize the total strain energy. From a numerical perspective, Kalker [13] formulate the minimization problem as a quadratic programming problem to solve frictionless non-Hertzian contact problems. The above two methods are based on the elastic half-space model [14] so that linear elasticity theory holds. For contact problems involving large deformation at contact, a more general approach, the *finite element method* (FEM), is widely used to analyze compliant grippers. However, its formulation is complicated and often requires intensive computation. Yin and Lee [15] proposed a numerical solver based on elliptical integrals to solve the problem of a large-deflected gripper contacting an elliptic object. By assuming only one contact point exists, the results agree well with those obtained by using FEM with less computation time. However, the solver models the gripper as a 1D segment without considering the thickness of the finger. Hence it is not applicable to thick fingers.

This paper presents an efficient computational model using nonlinear constrained optimization techniques to facilitate the design of compliant grippers. This model is rather general and

Manuscript received May 15, 2005. This work was supported in part by the Georgia Agricultural Technology Research Program (ATRP) and the U.S. Poultry and Eggs Association. C.-C. Lan is a Ph.D. Candidate in the Woodruff School of Mechanical Engineering at the Georgia Institute of Technology, Atlanta, Georgia 30332-0405, USA (e-mail: gtg032j@mail.gatech.edu)

*Corresponding author, K.-M. Lee is a Professor of the Woodruff School of Mechanical Engineering at the Georgia Institute of Technology, Atlanta, Georgia 30332-0405, USA (e-mail: kokmeng.lee@me.gatech.edu)

can be used to analyze contact between an arbitrarily shaped 2D object and a compliant gripper with arbitrary geometry in its lateral direction. Key to this model is the expression of strain energy and formulation of geometric constraints. This remaining paper offers the following:

1. *A formulation based on the Nonlinear Constrained Optimization (NCO) technique*. It offers a means to predict the deflected shape of the compliant gripper and its contact forces (both normal and tangential) with an object where the geometric shapes of the gripper cannot be ignored.
2. *Two classes of design configurations are considered*. namely, gripping with and without a rigid jaw as shown in Figs. 1(a) and 1(b) respectively. The former relies on indirect contact with the object through a jaw while in the latter the compliant gripper directly contacts the object.
3. *A numerical solver based on Sequential Quadratic Programming method.* This method solves the nonlinear constraint optimization problems.
4. *Verification with FEM*. We simulate two examples using the proposed method and compare the computed results against those obtained using FEM; the results are in excellent agreement with simpler formulation and much less computation effort.

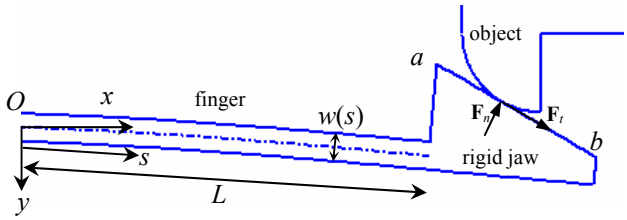

(a) Grip with a rigid jaw

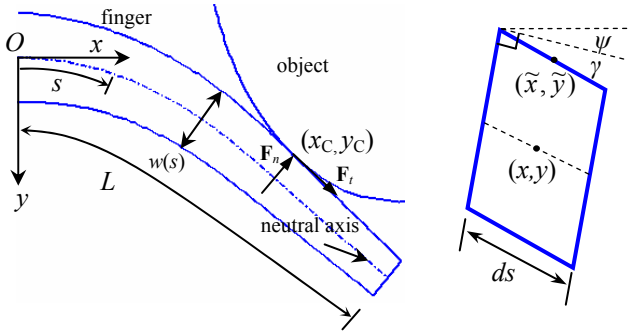

(b) Continuous grip without a rigid jaw (c) Differential segment

Fig. 1 Compliant gripping contacts

2. General Formulation of the Contact Problem

We formulate the compliant gripper contact problem as a constrained optimization problem. This begins with the strain energy expression of a compliant gripper capable of large deflection with shear deformation; followed by the formulation of geometric constraints that prevent the gripper from penetrating the object. The minimization of strain energy with geometric constraints together forms a nonlinear constrained optimization problem after discretization. Normal and tangential contact forces can be obtained by using the Newton's 3rd law.

2.1 Formulation of strain energy of the gripper

Consider the two classes of compliant grippers as shown in Fig. 1(a) and Fig. 1(b). The manipulation of grippers depends on the contact forces from the rigid object to make the fingers deflect in such a way that can accommodate the geometry of the object. The gripper shown in Fig. 1(a) has a triangular jaw attached at the end while the surface of the gripper in Fig. 1(b) is in direct contact with an elliptical object. Note that the shapes of the jaw and object are not restricted to the schematics shown in Fig. 1.

In order to characterize the gripper deflection, we generalize Timoshenko's beam theory [16] so that it can account for large flexural deflection with shear deformation. Timoshenko's beam theory is applicable to small deflections with assumptions that (a) the cross-section remains planar after deflection and (b) the gripper is inextensible. The deflection of a differential segment shown in Fig. 1(c) is interpreted as a superposition of two effects: (I) a bending moment induces an angle of rotation ψ without changing the shear angle, and (II) the shear force distorts the segment by a shear angle γ without causing it to rotate. The resultant of these effects is that the cross-section rotates by an angle $\psi+\gamma$. *Furthermore, by replacing the differential arc length ds with dx, we generalized Timoshenko's theory so that it is applicable to large deflections.* Since most deformation of the gripper is due to bending and shear, we neglect the local surface deformation (treat as rigid surface) and state the strain energy V stored in a deflected gripper as

$$V = \tfrac{1}{2}\int_0^L \left\{ EI(s)\left(\frac{d\psi}{ds}\right)^2 + \kappa GA(s)\left[\gamma(s)\right]^2 \right\} ds \qquad (1)$$

where s is an arc length;

A, L, and I are the cross-section area, length and moment of inertia of the gripper respectively;

E and G are respectively the Young's and shear moduli of the gripper;

ψ is the angle of rotation of the gripper;

γ is the shear angle of the gripper;

κ is the shear coefficient; and

$[x_C, y_C]^T$ is the position vector of the contact point.

The shear coefficient κ is introduced in order to correct the assumption (a) made above. In (1), the 1st and 2nd terms in the integral account for the strain energy due to bending and shear respectively. Here we perform a quasi-static analysis and assume that the gripper and object are on the verge to slip. Hence the magnitude of normal force $|\mathbf{F}_n|$ and contact force $|\mathbf{F}_t|$ are related to each other by $\mu|\mathbf{F}_n|=|\mathbf{F}_t|$ where μ is kinetic friction coefficient. Since the virtual work due to normal and friction force is canceled between the gripper and object, the potential energy of the system only includes (1).

From hereafter we set the x-axis pointing to the undeflected direction of the gripper and y-axis to the deflected direction. The dash line in the middle of the finger represents the neutral axis and the position of a point (x, y) on it can be obtain as

$$\begin{bmatrix} x \\ y \end{bmatrix} = \int_0^{\hat{s}} \begin{bmatrix} \cos(\psi+\gamma) \\ \sin(\psi+\gamma) \end{bmatrix} ds \qquad (2)$$

where $\hat{s}$ is the arc length from origin O to point (x, y).

2.2 Formulation of geometric constraints

The geometric constraints are formulated in order to describe the state at contact. Specifically, the points $(\tilde{x}, \tilde{y})$ on the contact surface of the gripper must satisfy the following inequality in order not to penetrate the rigid object

$$g(\tilde{x}, \tilde{y}) \geq 0 \tag{3}$$

where $g(x,y)=0$ describes the surface of the object that contacts the gripper. Depending on the location of contact, the points $(\tilde{x}, \tilde{y})$ on the contact surface for the two classes of grippers can be stated as follows.

Case I: Compliant finger with a rigid jaw (indirect contact)

Since the local deformation near contact area of the jaw is small compared with the deflection of the finger, it can be treated as a rigid body. The position $(\tilde{x}, \tilde{y})$ of a point on the surface of the jaw, i.e., line segment *ab*, can be described by the angle of rotation at $s=L$ and the point $[x(L), y(L)]$.

$$\begin{bmatrix} \tilde{x} \\ \tilde{y} \end{bmatrix} = \begin{bmatrix} x_L \\ y_L \end{bmatrix} + \begin{bmatrix} \cos(\psi_L + \gamma_L) & \sin(\psi_L + \gamma_L) \\ -\sin(\psi_L + \gamma_L) & \cos(\psi_L + \gamma_L) \end{bmatrix} \begin{bmatrix} P_x \\ P_y \end{bmatrix} \tag{4}$$

where the subscript L denotes the value obtained at $s=L$; and $[P_x, P_y]^T$ is the position vector from (x_L, y_L) to $(\tilde{x}, \tilde{y})$ in the jaw frame (with origin at $[x_L, y_L]^T$ and axes parallel to *x-y* before contact);

Case II: Direct contact between compliant finger and object

When the finger surface is in direct contact with the object, an arbitrary point $(\tilde{x}, \tilde{y})$ on the contact surface of the finger can be related to its corresponding point on the neutral axis by

$$\begin{bmatrix} \tilde{x} \\ \tilde{y} \end{bmatrix} = \begin{bmatrix} x \\ y \end{bmatrix} + \frac{w(s)}{2} \begin{bmatrix} \sin(\psi + \gamma) \\ -\cos(\psi + \gamma) \end{bmatrix} \tag{5}$$

where $w(s)$ is the thickness of the finger.

2.4 Determination of normal and tangential contact forces

Of all the points on the contact surface, the one that satisfies the surface function $g=0$ is denoted as $\mathbf{P}_C=[x_C\ y_C]^T$. The contact force can be obtained by applying Newton's 3rd law at the gripper. Specifically, the contact forces $\mathbf{F}=[x_C\ y_C]^T$ from the gripper to the object (or $-\mathbf{F}$ from the object to the gripper) must have a moment on the gripper that equals the reaction moment at *O*.

$$EI(s)\left.\frac{d\psi}{ds}\right|_{s=0} = -\mathbf{P}_C \times \mathbf{F} \tag{6}$$

The contact force $\mathbf{F}$ includes normal and tangential components that can be written in the following form.

$$\mathbf{F} = [F_x\ F_y]^{\mathrm{T}} = \mathbf{F}_n + \mathbf{F}_t = [F_{nx}\ F_{ny}]^{\mathrm{T}} + [F_{tx}\ F_{ty}]^{\mathrm{T}} \tag{7}$$

The direction of normal contact force must be parallel to the gradient of the object surface at $(x_C\ y_C)$.

$$\left.\frac{\partial g / \partial y}{\partial g / \partial x}\right|_{(x_C, y_C)} = \frac{F_{ny}}{F_{nx}} \tag{8}$$

Since normal contact force and tangential (friction) contact force are orthogonal to each other, we have

$$F_{nx} F_{tx} = F_{ny} F_{ty} \tag{9}$$

Since the contact surface is on the verge to slip, the magnitude of normal force relates to the magnitude of friction force by

$$\mu \sqrt{F_{nx}^2 + F_{ny}^2} = \sqrt{F_{tx}^2 + F_{ty}^2} \tag{10}$$

where μ is the kinetic friction coefficient. The components F_{nx}, F_{ny}, F_{tx}, and F_{ty} can be solved simultaneously from (6), (8), (9), and (10). Note that the signs of F_{tx} and F_{ty} have to be determined from the direction of interaction between the gripper and object.

2.5 Numerical discretization

In order to obtain the deflected shape of the gripper, we apply the principle of minimum potential energy for (1) with geometric constraints (3). Specifically, the principle of minimum potential energy states that of all admissible displacements, those that satisfy the equilibrium condition at contact make the total potential energy minimum. Namely, we are trying to find the minimum of V from (1) with the admissible displacements imposed by (3). Rather than seeking a closed-form solution, we resort to numerical approximations by discretizing the neutral axis of the finger into N equally spaced intervals and the contact surface into M equally spaced intervals. We use capital letters to denote the approximated values of the variables.

$$\begin{aligned} &s_i = i\Delta s\ ,\ \Delta s = {}^{L}\!/_{N}\ ,\ i = 0 \sim N \\ &\Psi_i \approx \psi_i = \psi(s_i)\ ;\ \Gamma_i \approx \gamma_i = \gamma(s_i)\ ,\ i = 0 \sim N \\ &X_i \approx x_i = x(s_i)\ ;\ Y_i \approx y_i = y(s_i)\ ,\ i = 0 \sim N \\ &\tilde{X}_j \approx \tilde{x}_j = \tilde{x}(s_j)\ ;\ \tilde{Y}_j \approx \tilde{y}_j = \tilde{y}(s_j)\ ,\ j = 0 \sim M \end{aligned} \tag{11}$$

Hence we can approximate (1) by, but not restricted to, the trapezoidal rule.

$$V \approx \tfrac{1}{2}\Delta s \left[\sum_{i=1}^{N} EI_{i+1/2} \left(\frac{\Psi_i - \Psi_{i-1}}{\Delta s} \right)^2 + GA_{i+1/2} \left(\frac{\Gamma_i + \Gamma_{i-1}}{2} \right) \right] \tag{12}$$

The area A and moment of inertia I are approximated as

$$I_{i-1/2} = \frac{I(s_i) + I(s_{i-1})}{2}\ ;\ \text{and}\ \ A_{i-1/2} = \frac{A(s_i) + A(s_{i-1})}{2} \tag{13}$$

Since the gripper is clamped at the base, the initial angle of rotation (ψ_0) and position (x_0, y_0) are equal to zero.

$$\Psi_0 = 0\ ;\ X_0 = 0\ ;\ \text{and}\ Y_0 = 0 \tag{14}$$

Follow from (2), any point on the neutral axis of the finger can be approximated as

$$\begin{aligned} X_i &= \tfrac{1}{2} \sum_{k=0}^{i-1} \left[\cos(\Psi_k + \Gamma_k) + \cos(\Psi_{k+1} + \Gamma_{k+1}) \right] \Delta s \\ Y_i &= \tfrac{1}{2} \sum_{k=0}^{i-1} \left[\sin(\Psi_k + \Gamma_k) + \sin(\Psi_{k+1} + \Gamma_{k+1}) \right] \Delta s \end{aligned} \tag{15}$$

where $i=1 \sim N$. The points on the contact surface can be obtained by plugging (15) into (4) or (5). The approximated $(\tilde{X}, \tilde{Y})$ is then substituted into (3)

$$g_j(\tilde{X}_j, \tilde{Y}_j) \geq 0\ ;\ j = 1 \sim M \tag{16}$$

Equation (12) is a quadratic object function that has to be minimized subject to the constraint functions from (16) with independent variables Ψ_i and Γ_i $(i=1 \sim N)$. The numerical solvers for obtaining the optimal solution will be presented in Section 3. Note that the number of intervals M for the neutral axis, in general, does not have to be equal to the number of intervals N of the contact surface.

3 Sequential (Successive) Quadratic Programming (SQP)

In this section we introduce a numerical algorithm based on sequential quadratic programming (SQP) to solve the optimization problem governed by (12) and (16). The general nonlinear minimization problem with inequality constraints can be stated as follows.

$$\begin{aligned} &\min\ f(\mathbf{x}) \\ &\text{subject to}\ g_i(\mathbf{x}) \ge 0\,,\ i = 1 \sim M \end{aligned} \tag{17}$$

where g_i is the i^{th} inequality constraint function.

The idea of SQP is to approximate the current state (say, $\mathbf{x}_k$) by a quadratic programming (QP) sub-problem as

$$\begin{aligned} &\min\ \tfrac{1}{2}\mathbf{p}^T\nabla^2 L(\mathbf{x}_k)\mathbf{p} + \nabla f_k^T\mathbf{p} \\ &\text{subject to}\ \nabla g_i(\mathbf{x}_k) + g_i(\mathbf{x}_k) \ge 0\,,\ i = 1 \sim M \end{aligned} \tag{18}$$

where $\mathbf{p} = \mathbf{x} - \mathbf{x}_k$ and $L = f(\mathbf{x}) + \sum_{i=1}^{m} \lambda_i g_i(\mathbf{x})$

Equation (18) contains a quadratic approximation of $f(\mathbf{x})$ and linear approximations of $g_i(\mathbf{x})$. The minimizer of (16) is then used to define a new state by setting $\mathbf{x}_{k+1} = \mathbf{x}_k + \mathbf{p}$. The minimizer of the QP should be the optimal solution of (17) when the iterative process converges. The disadvantages of SQP are that the computation of Hessian matrix $\nabla^2 L(\mathbf{x}_k)$ is time-consuming for large problems and that it may not be positive definite. Various quasi-Newton algorithms can be used to approximate Hessian matrix. Here we adopt the popular BFGS algorithm (by Bryoden, Fletcher, Goldfarb, and Shanno). The formulae are states as follows [17].

$$\widetilde{\mathbf{W}}_{k+1} = \widetilde{\mathbf{W}}_k + \frac{\mathbf{q}_k\mathbf{q}_k^T}{\mathbf{q}_k^T\mathbf{p}_k} - \frac{\widetilde{\mathbf{W}}_k\mathbf{p}_k\mathbf{p}_k^T\widetilde{\mathbf{W}}_k}{\mathbf{p}_k^T\widetilde{\mathbf{W}}_k\mathbf{p}_k} \tag{19}$$

where

$$\mathbf{p}_k = \mathbf{x}_{k+1} - \mathbf{x}_k \tag{19a}$$

and

$$\mathbf{q}_k = \nabla f(\mathbf{x}_{k+1}) - \nabla f(\mathbf{x}_k) + \nabla\sum_{i=1}^{m} \lambda_{k+1,i}\left[g_i(\mathbf{x}_{k+1}) - g_i(\mathbf{x}_k)\right] \tag{19b}$$

$\widetilde{\mathbf{W}}_{k+1}$ is the approximation Hessian for the next step. The steps for the SQP are outlined as below.

Computational steps

Given initial $\mathbf{x}_0$, $\widetilde{\mathbf{W}}_0$, $\lambda_{0,i}$ (i=1~m), $\beta \in [0,1]$, and tolerance ε:

1. Solve (18) for $\mathbf{p}$ and $\lambda_{k+1,i}$ (i=1~m)
2. For k=0,1,2…
   - Set $\mathbf{x}_{k+1} = \mathbf{x}_k + \beta\mathbf{p}$
   - While $f_{k+1} > f_k$
     - $\mathbf{x}_{k+1} = \mathbf{x}_k + \beta(\mathbf{x}_{k+1} - \mathbf{x}_k)$
   - End
   - Obtain BFGS update matrix $\widetilde{\mathbf{W}}_{k+1}$ from (19).
   - If $|f(\mathbf{x}_{k+1})| < \varepsilon$, exit

End

4 Verification of Frictionless and Frictional Contact

In this section we illustrate with two examples to verify the NCO technique introduced in Section 2. In Example I, we consider an indirect gripping contact where the object contacts with the gripper through a triangular jaw. In Example II the direct contact of the gripper with an elliptical object is considered. The simulation results are then compared against those obtained by using FEM. Both frictionless and frictional contacts will be considered. Note that in Example I we need not consider shear deformation since finger thickness is relatively small.

Example I: Passive gripper for micro-assembly

The assembly process using a compliant gripper includes insertion, deflection, and assembly. An effective assembly requires designing the geometry of the gripper and its jaw such that it is easy to insert but very difficult to pull out. For clarity, we consider in Fig. 2 a gripper with a triangular jaw and a circular object surface. Due to symmetry, only half of the gripper needs to be considered.

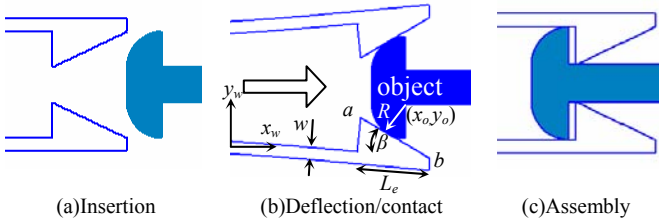

(a)Insertion (b)Deflection/contact (c)Assembly

Fig. 2 Gripper assembly sequence

Since only segment *ab* on the jaw contacts with the object, we only need to discretize surface *ab* into M equally spaced intervals. The geometric constraints can be obtained by using the equation of a circle

$$g_j(\widetilde{X}_j, \widetilde{Y}_j) = (\widetilde{X}_j - x_o)^2 + (\widetilde{Y}_j - y_o)^2 - R^2 \ge 0 \tag{20}$$

where R is the radius of the extrusion part of the object and (x_o, y_o) is the center of the circle as shown in Fig. 2(b). The simulation parameters for both the NCO technique and FEM are listed in Table 1. Figs. 3 and 4 show the forces required as the gripper inserts into the fixture. The NCO technique matches well with FEM with differences less than 3%. Figure 5 also shows the deflection shape obtained by ANSYS where x_o= 0.06781m. The comparison of computation time of this particular result in Table 2 shows that the NCO technique is more efficient than FEM without losing accuracy.

Table 1 Simulation parameters and values

Parameters	Values	Parameters	Values
Young's modulus(N/m^2)	2.6x10^9	element type for ANSYS	PLANE2 for both gripper and object
Lead angle β	25°		
Thickness w	0.0032m		
Width b	0.0095m	# of elements for ANSYS	1266
Finger length L	0.057m		
Jaw length L_e	0.019m	N	100
Fixture radius R	0.0089m	M	100
Fixture position y_o	0.0105m		

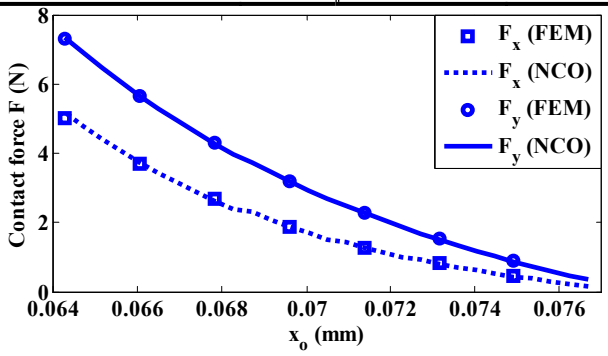

Fig. 3 Simulation result of a gripper assembly (μ=0)

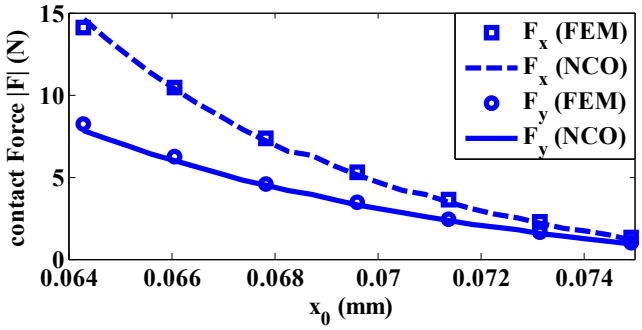

Fig. 4 Simulation result of a gripper assembly (μ=0.5)

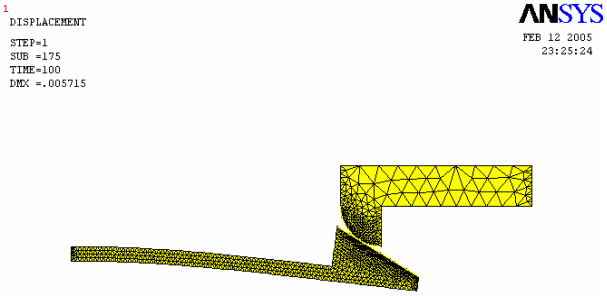

Fig. 5 Simulation results from FEM

Table 2 Comparison of computation time

Method	Time(sec)
NCO(without shear deformation)	20.95
FEM(ANSYS)	516.463

Example II: Gripper for object handling

In this example we illustrate an application where the gripper manipulates an object by direct contact through finger. The finger needs to make contact with the object. For ease of illustration, we consider a case where a nonuniform gripper manipulates an elliptical object as shown in Fig. 6. We perform a quasi-static analysis where the relationship between the moving object and rotating finger can be described by

$$\phi = -236.22x_e + 102^\circ \qquad (21)$$

where x_e is in meters and ϕ is the rotation between gripper frame xy and world frame $x_w y_w$. The contact surface includes one side of the finger that approaches the object. Since the contact location is unknown, the whole finger surface needs to be discretized and the geometric constraints can be obtained by using the equation of an ellipse.

$$g_j = b_1\tilde{X}_j^2 + b_2\tilde{Y}_j^2 + b_3\tilde{X}_j\tilde{Y}_j + b_4\tilde{X}_j + b_5\tilde{Y}_j + b_6 \geq 0 \qquad (22)$$

where b_i's are the coefficients of the elliptical object

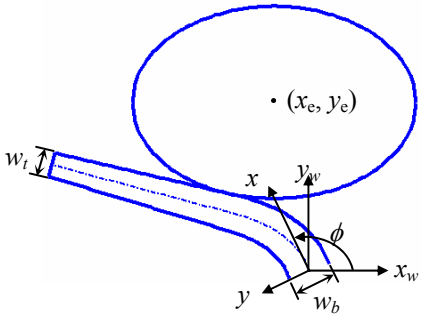

Fig. 6 Schematics of a rotating gripper contacting an object

As mentioned in Section2, Timoshenko's beam theory includes a shear coefficient κ. Various shear coefficient formulae have been proposed. As shown in (23), we adopt the shear coefficient formula suggested by Kaneko [18] to correct the shear angles of grippers with rectangular cross section.

$$\kappa = (5+5\nu)/(6+5\nu) \qquad (23)$$

where ν is Poison's ratio. We again compare the results of the NCO technique with FEM. Simulation parameters are listed in Table 3. Figure 7 shows the continuous snapshots where the object moves from left to right while the gripper rotating clockwise. The computation time of x_e=0.0508m is compared in Table 4. In Fig. 8 we compare the results of frictionless contact by using the NCO technique, FEM and one-dimensional model (treat finger as a line segment). In Fig. 9, the results of frictional contact are also compared with direction of friction force pointing to the positive x axis.

Table 3 Simulation parameters and values

Parameters	Values	Parameters	Values
Young's modulus	4.8×10^6 N/m^2	element type for ANSYS	PLANE2 for ellipse and PLANE42 for gripper
Shear modulus	1.71×10^6 N/m^2		
Poison's ratio	0.4		
Base thickness w_b	0.030m	# of elements for ANSYS	1080
Tip thickness w_t	0.017m	N	90
Width b	0.025m	M	90
Ellipse long axis	0.09906m		
Ellipse short axis	0.06731m		
Ellipse position y_e	0.12065m		

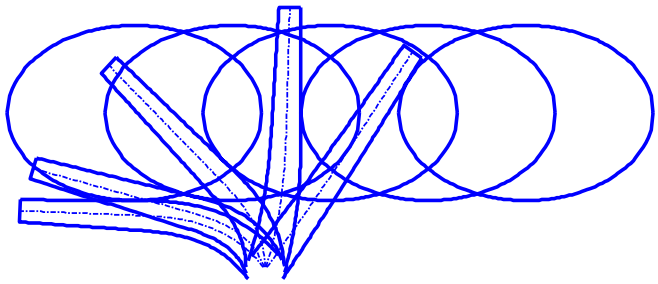

Fig. 7 Snapshots of gripper-ellipse contact (ϕ=126°, 108°, 90°, 72°, 54° from left to right)

Table 4 Comparison of computation time

Method	Time(sec)
NCO(without shear deformation)	15.352
NCO(with shear deformation)	33.358
FEM(ANSYS)	222.42

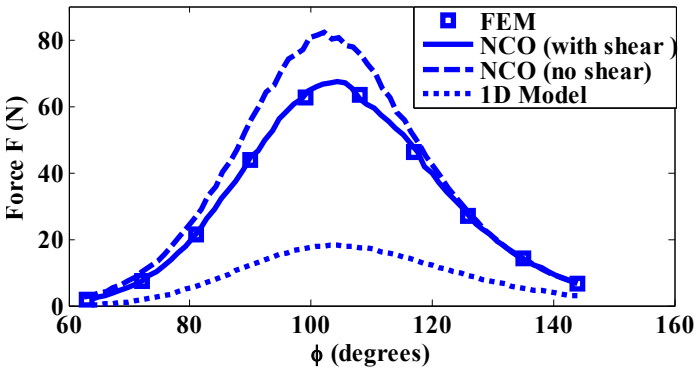

Fig. 8 Comparison of simulation results (μ=0)

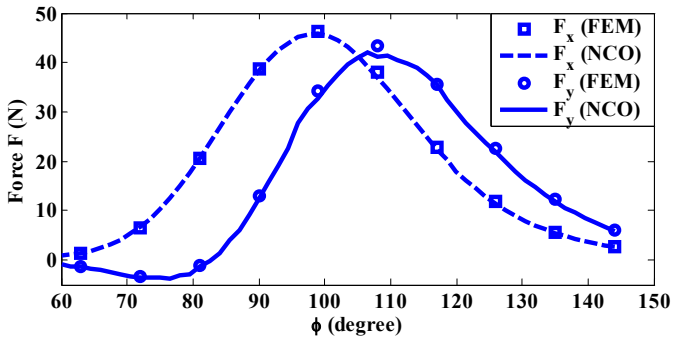

Fig. 9 Comparison of simulation results (μ=0.5)

The following observations can be made from the comparison between COM and other existing methods:

1. The one-dimensional model, which treats the finger as a line segment, ignores the geometry of the finger hence is only applicable for fingers with relatively small thickness. The error of contact forces will increase as the thickness increases.
2. When applying the NCO technique without considering shear deformation of the gripper, the error increases as contact force increases. The overall contact forces also tend to be higher than those with considering shear deformation. When considering shear deformation, the predicted contact forces obtained from the NCO technique matches well with FEM. Typical differences are within 3%. Without losing accuracy, the NCO technique, which discretizes the finger in one dimension (along the neutral axis), is far faster than FEM which discretizes the gripper in two dimensions (along the neutral axis and transverse direction).
3. The excellent agreement of the NCO technique and FEM also verifies that the assumption of small surface deformation is valid for frictionless contact and frictional contact with moderate friction coefficient.
4. In order to satisfy the boundary conditions of gripper/object surface, FEM requires discretization of both gripper and object surface while the NCO technique only needs to discretize the gripper surface. Hence the formulation of NCO can be simpler.

5 Conclusions

A computational model based on Nonlinear Constrained Optimization (NCO) techniques has been presented for analyzing compliant grippers whose manipulation relies on direct or indirect contact with the objects. The model takes into account large flexural deflection and shear deformation whose effect can not be neglected for thick fingers. By formulating geometric constraints this model can be applied to nonuniform fingers and jaws with arbitrary geometry.

Two types of compliant grippers have bee presented to illustrate the formulation. Both frictionless and frictional contacts have been considered. The simulation results of NCO technique agree well with those obtained by using FEM with difference typically within 3%. Compared with FEM, the advantages of the NCO technique are the following: (a) The dimension of discretization can be reduced by one, namely, 2D problem can be reduced to 1D and 3D problem can be reduced to 2D. Hence it is computationally much more efficient than FEM. (b) The object domain need not be discretized. Hence its formulation is simpler than FEM.

The excellent agreement shows that the formulation and analysis offered by the NCO technique can effectively facilitate the process of design and optimization of compliant grippers that have a broad spectrum of applications ranging from MEMS device fabrication [8] to automated handling of live objects in food processing industry [2]. The formulation can also be further extended to compliant grippers with external actuators.

References

[1] Bonenberger, P. R., 2000, *The First Snap-Fit Handbook: Creating Attachments for Plastics Parts*, Hanser Gardner Publications.

[2] Lee, K.-M., R. Carey, M. Lacey, and B. Webster, 1996, "*Automated Singulating System for Transfer of Live Broiler*," Proposal to US Poultry and Egg Association.

[3] Lee, K.-M., 1999, "On the Development of a Compliant Grasping Mechanism for On-line Handling of Live Objects, Part I: Analytical Model," *Int. Conf. on Advanced Intelligent Mechatronics Proc.*, Atlanta, September 19-23, pp. 354-359.

[4] Salim, R., Wurmus, H., Harnisch, A., and Hulsenberg, D., 1997, "*Microgrippers created in microstructurable glass,*" Microsystems Technology, **4,** pp. 32-34.

[5] Kim, C.J., Pisano, A., and Muller, R., 1992, "*Silicon-processed overhanging microgripper*," Journal of Microelectromechanical Systems, **1**, pp.31-36.

[6] Suzuki, Y., 1996, "*Flexible Microgripper and its Application to Micro-Measurement of Mechanical and Thermal Properties*," IEEE MEMS Proceedings 9th Annual International Workshop, pp.406-411.

[7] Ansel, Y., Schmitz, F., Kunz, S., Gruber, H. P., and Popovic, G., 2002, "Development of Tools for Handling and Assembling Microcomponents," Journal of Micromechanics and Microengineering, **12**, pp.430-437.

[8] Tsui, K., Geisberger, A. A., Ellis, M., Skidmore, G. D., 2004, "*Micromachined End-effector and Techniques for Directed MEMS Asembly*," J. Micromech. Microeng., **14**, pp. 542-549.

[9] Oh, Y. S., Lee, W. H., Skidmore, G. D., 2003, "*Design, Optimization, and Experiments of Compliant Microgripper*," ASME IMECE, Washington, D. C.

[10] Paul, B., Hashemi, J., 1981, "*Contact Pressure on Closely Conforming Elastic Bodies*," ASME J. of Applied Mechanics, **48,** pp. 543.

[11] Fichera, G., 1964, " Problemi elastostatici con vincoli unilaterale: il problema di Signorini con ambigue condizioni al contorno," Mem. Accad. Naz. Lincei, Series 8, **7,** pp. 91.

[12] Duvant, G., Lions, J. L., 1972, Les Inequations en Mecanique et en Physique, Dunod, Paris.

[13] Kalker, J. J., van Randen, Y., 1972, "*A minimum Principle for Frictionless Elastic Contact with Application to non-Hertzian Half-space Contact Problems*," J. Eng. Mathematics, **6**, pp. 193.

[14] Johnson, K. L., 1987, *Contact Mechanics*, Cambridge Univesity Press.

[15] Yin, X., K-M. Lee, 2002, "*Modeling and Analysis of Grasping Dynamics of High Speed Transfer of Live Birds*," 2nd IFAC Conference on Mechatronic Systems, Berkeley, CA, USA.

[16] Timoshenko, S. P., 1922, "*On the Transverse Vibrations of Bars of Uniform Cross-Section*," Philosophical Magazine, VI, 43, pp.125-131.

[17] Bazaraa, M.S., Sherali, H.D., and Shetty, C.M., 1993, *Nonlinear Programming: Theory and Algorithms*, John Wiley & Sons, Inc., New York, NY.

[18] Kaneko, T., 1975, "*On Timoshenko's Correction for Shear in Vibrating Beams*," J. Phys. D: Appl. Phys., **8**, pp. 1927-1936.